Diffraction and multichannel specular reflection of conduction electrons from a metal surface

P. P. Lutsishin, T. N. Nakhodkin, O. A. Panchenko, and Yu. G. Ptushinskiĭ

Institute of Physics, Academy of Sciences of the Ukrainian SSR, Kiev

The influence of submonolayer ordered impurity films of oxygen, hydrogen, and silver on the nature of the reflection of conduction electrons from the surface of thin single-crystal tungsten plates ordered in the (110) plane has been investigated. The symmetry of the adsorbed layers was monitored by the method of low-energy electron diffraction; the nature of the reflection of conduction electrons by the static skin-effect technique. It is shown that the interaction of conduction electrons with a surface covered with an ordered film is diffractive. Cases of multichannel specular reflection by the metal boundary were studied in detail; there are then several nonequivalent states for specular reflection of electrons. The relation between the tangential components of the quasimomenta of incident and reflected electrons is determined by the Bragg relation. Specularly reflected electrons are then transferred both to physically equivalent points in phase space and to other sheets of the Fermi surface. It is shown that such transitions (electron-hole umklapp processes) can be "switched-on" depending on the translational symmetry of the adsorbed film or during rotations of the inverse lattice surfaces relative to the axes of the crystal substrate. The film symmetry varied as a result of a change in concentration of impurity atoms.

PACS numbers: 73.40.Jn, 73.40.Ns, 72.15.Qm

INTRODUCTION

The adsorption of submonolayer impurity films has an appreciable influence on the nature of the reflection of conduction electrons at macroscopically smooth surfaces of metal crystals. This is indicated by recent experimental investigations using the static skin-effect[1-6] and electron focusing,[7,8] as well as by some other work.[9,10] These results show that an adsorbed disordered monatomic layer increases the diffuse background. An increase in diffuseness is not, however, the only possible way in which the nature of the surface reflection of electrons can change.

In fact, submonolayer films often form ordered two-dimensional structures with symmetry determined by the choice of adsorbate-adsorbent system, by the surface concentration of impurity atoms, and by the temperature. Every new surface structure can then be associated with definite selection rules for the wave-vector of the scattered waves

$$k_t' = k_t + ng, \tag{1}$$

which connect the tangential components of the quasimomenta of the incident, k_t, and reflected, k_t', electrons by the well known Bragg relation. Equation (1) can also be regarded as one of the forms of the momentum conservation law in the crystal. The conditions for diffraction and specular reflection are satisfied on the straight line $k_t = $ const (or $g = $ const), which repeat periodically in the reciprocal lattice with period g, while $n = 1, 2, \ldots$ determines the order of the diffraction. Depending on the phase state of the adsorbed film (and consequently on the fully determined magnitude of the two-dimensional vector g), the reflection of electrons can be either close to specular, can exhibit features of multichannel specular reflection, or can be diffuse.[11,12]

Umklapp processes are evidently the clearest consequence of diffraction of electrons by two-dimensional surface gratings. Umklapp processes can be "switched-on" by the corresponding choice of structure or orientation of the adsorbed layer. They are revealed by the method of electron focusing[13] and also have an appreciable influence on size effects in the kinetic properties of metals,[14] especially on the static skin effect.[15-18]

The present work is devoted to a study of the effect of ordered adsorbed films of oxygen, hydrogen and silver on the static skin effect in thin tungsten plates. We have published preliminary results for the oxygen-tungsten system earlier[18].

EXPERIMENTAL METHOD

All measurements were carried out for the basal plane (110) of tungsten crystals. The method of low-energy electron diffraction (LEED)[19] was used to monitor the surface state of the specimens. The nature of the reflection of electrons and its variation under the influence of adsorption was determined by the static skin-effect method. The measurements were made at low temperatures under high vacuum. The experimental vacuum equipment included for this an LEED system, a system for cooling and temperature control of the specimen, a source of impurity atoms, a cooled getter pump, and a manometer. A schematic diagram of the apparatus is shown in Fig. 1. An electromagnet with electronic field stabilization provided the magnetic field.

The starting material for preparing the specimens, in the shape of thin plates, consisted of ingots of pure single-crystal tungsten with the ratio $\rho(300 \text{ K}/\rho(4.2 \text{ K})$ $\approx 1.3 \times 10^5$. The specimen thickness was 120 to 135 μm with the other dimensions 3×10 mm. Their shape in plan is shown on the inset to Fig. 1. The specimens were hung in vacuum on 0.3 mm diameter tungsten threads, welded to fairly massive 2 mm diameter molybdenum leads which were led through a glass seal to
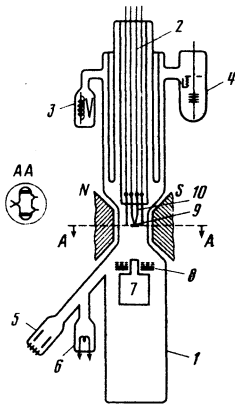
FIG. 1. Sketch of experimental high-pressure apparatus: 1—glass vessel, 2—stem for liquid helium, 3—manometer, 4—cooled "orbitron" getter pump, 5,6—oxygen, hydrogen and silver sources, 7—electron gun, 8—system for holding grid and screen, covered with a phosphor, 9—specimen, 10—thermocouple. The inset shows a plane view of the specimen.

the helium part of the cryostat. This suspension enabled the specimens to be heated to 2500 K for cleaning the surface or to be cooled to $T \approx 4.2$ K when measuring the magnetoresistance. We have described earlier[4,5] the procedure for preparing the surface. In the present work more attention was paid than ever before to removing the carbon impurity from the surface, using Becker's method.[20] The carbon was removed in an oxygen atmosphere ($P \sim 2 \times 10^{-6}$ mm Hg) at $T = 1900$ K for 20 h. As a result of this, the magnetoresistance of the cleaned plates remained unaltered during the whole measuring cycle, including repeated deposition of surface films and their removal. The number of such depositions reached the order of thousands. Less thorough removal of carbon leads to its accumulation in subsurface regions and to a gradual change in the specimen characteristics.

A strong magnetic field $H = 7.5$ kOe ($\omega\tau \gg 1$, where ω is the cyclotron frequency and τ the relaxation time) was directed in the plane of the thin specimen ($d < l$, where l is the mean free path and d the plate thickness) and was perpendicular to the dc current flowing through the specimen ($H \perp I$, $I \leq 4$ A). The specimen resistance R in a magnetic field or the variation ΔR with exposure time or with temperature was recorded automatically or measured point by point using an R-348 potentiomater.

Low temperatures provide the most important condition for observing the static skin effect, for the inequalities $\omega\tau \gg 1$ and $l > d$ are then satisfied. Cooling of the specimens to close to liquid helium temperature was achieved by the heat conductivity of the molybdenum leads. Their length was about 5 cm and the specimen temperature, measured with a W + 5% Re–W + 20% Re thermocouple did not differ from 4.2 K by more than 0.1 K. Indirect evidence confirms these estimates. For example, Fig. 2 shows the dependence of the magnetoresistance of a plate for two states of the surface (atomically pure and covered with an oxygen film) on the time after the boiling of the helium in the cryostat. This moment is marked in the figure by the vertical
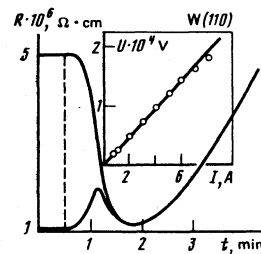

FIG. 2. The variation of the magnetoresistance of the specimen $R(t)$ after boiling of the liquid helium in the cryostat; this moment is indicated by the dashed line; $H = 7.5$ kOe. The upper curve corresponds to the case of the crystal surface being covered with an oxygen film with the (2×2) structure. The lower curve corresponds to an atomically clean surface. The inset shows the voltage drop U along the specimen as a function of the measuring current I for $H = 7.5$ kOe. Linearity is preserved at $I \leq 5$ A.

dashed line. Even after 30 s the magnetoresistance and consequently its temperature starts to fall noticeably. Both curves pass through all the stages known from direct measurement of $R(T)$ at $H = 7.5$ kOe.[21-23] The deep minimum corresponds to the condition $\omega\tau \approx 1$ which is satisfied at $T \approx 30$ K and the maximum on the lower curve corresponds to $T \approx 15$ K. The static skin-effect regime[22] is established at $T < 30$ K. One sees the rather high sensitivity of R to the state of the specimen surface; deposition of an oxygen film leads to a fivefold increase in R in the present case. The inset to Fig. 2 shows the voltage drop across the specimen as a function of the current flowing through it. The departure from linearity indicates, apparently, heating of the specimen in the applied magnetic field $H = 7.5$ kOe.

The LEED system consisted of a standard electron gun with the beam energy variable in the range from 10 to 100 eV at a beam current of 0.5 to 1.5 A. An important condition for its operation was accurate cancellation of the stray fields of the electromagnet. The usual filtering of inelastically scattered secondary electrons and a luminescent screen on which the diffraction picture was shown were employed in the apparatus.

The adsorbate and the cooled "orbitron" getter pump were placed in separate containers connected to the main volume of the vacuum system. The oxygen source was copper oxide heated to dissociation, and the hydrogen source was a titanium coil previously saturated with hydrogen. The silver was sputtered from a special crucible. All the sources were prepared and treated during pumping by standard methods which achieved high purity of the deposited material during the measurements. The vacuum in the experimental apparatus was, according to an Alpert gauge, maintained at $\sim 10^{-10}$ mm Hg. During deposition on the surface, the partial pressure of oxygen or hydrogen was $\sim 10^{-6}$ mm Hg.

EXPERIMENTAL RESULTS AND DISCUSSION

Oxygen-tungsten system. Oxygen was adsorbed on a tungsten (110) face at a temperature $T = 700$ K. By this means a monolayer covering was obtained in spite of the rapid reduction in the rate of surface condensation

of the oxygen. Intermediate surface concentrations of oxygen were obtained by the choice of exposure time. No monolayer coating was produced within a reasonable experimental period at lower adsorption temperatures.[18]

The dependence of the magnetoresistance of a thin plate on the exposure time in an oxygen atmosphere, $R(t)$, which characterizes the surface scattering of electrons over the whole coating range Θ $(0 \leqslant \Theta \leqslant 1)$, is shown in Fig. 3. R was measured in a fixed magnetic field $H = 7.5$ kOe after a certain surface concentration of oxygen had been reached. The measuring procedure amounted to the following: after a certain fraction of the material had been deposited, the oxygen partial pressure in the apparatus was reduced, the specimen cooled to a temperature of 4.2 K, and the next value of R in a fixed magnetic field H was measured. New amounts of material were deposited on the cleaned crystal surface. In this way the heating time of the oxygen source could be taken into account.

A feature of the magnetoresistance curve $R(t)$ is the sharp increase in R in the region of low surface concentrations. The appearance of the first structure visible on the screen of the electron diffraction camera corresponds to a fall in R. According to accepted terminology,[24] this structure is denoted by the symbol $p(2 \times 1)$. The maximum development of this structure, i.e., the clearest diffraction reflections, corresponds to the minimum in R. The whole region of existence of the $p(2 \times 1)$ structure is indicated in the figure by vertical lines. Further increase in the surface concentration of oxygen leads to a change in structure from $p(2 \times 1)$ to (2×2) and to the appearance of a maximum in R at the greatest brightness of the LEED picture. The transition to a multilayer is accompanied by the disappearance of all additional diffraction reflections and to a smooth reduction in R to the original value for a clean tungsten surface. A series of Laue pictures from two-dimensional structures, obtained during the course of this experiment, is shown in Fig. 4. The first corresponds to a pure metal surface. The additional reflections for the two following structures appear without any noticeable change in the brightness of the basic ones. The diffraction picture returns to the initial appearance

FIG. 4. Successive diffraction patterns for the oxygen-tungsten system: a—clean crystal surface [(110) face], b—$p(2 \times 1)$ structure, c—(2×2) structure. Primary electron beam energy $E = 30$ eV.

upon transition to a monolayer and is not shown in Fig. 4. We also note that adsorption of oxygen on a crystal cooled to 4.2 K does not lead to the formation of any ordered structures visible on the screen, while the resistance increases slowly to saturation.[18]

We shall consider some features of two-dimensional diffraction gratings formed by adsorbed oxygen atoms. We note first of all that LEED is a direct method for determining the symmetry of adsorbed layers, but gives only indirect information (or none whatever) about the position of the adsorbed particles on the metal surface.[25] Cases of reconstructive adsorption, i.e., the shift of the basic atoms under the influence of the impurities, can also only be deduced with great difficulty by invoking additional experimental results. It should be pointed out in this connection that results on the symmetry of surface gratings are quite sufficient for explaining the $R(\Theta)$ dependences which interest us. The structure interpretation shown in Fig. 5 is thus of a purely schematic form. We should point out that many experimental results obtained in recent years for the oxygen $+$ (110) tungsten face system indicate the absence of reconstructive adsorption at moderate specimen temperatures.[26-28] The first ordered structure is shown in Fig. 5, a and b; it is observed in the region of $\Theta = \frac{1}{2}$. The lattice is formed by closely packed rows of oxygen atoms drawn out along the $\langle \bar{1}11 \rangle$ or $\langle 1\bar{1}1 \rangle$ directions. There are empty spaces equal to a single lattice constant between the rows. Both orientations are present on a crystal surface and form a system of domains with linear dimensions not greater than the diameter of the LEED primary-electron beam. Thanks to this the different domains give comparable contributions to the brightness of the diffraction reflections.

The origin of the $p(2 \times 1)$ structure is important for us in interpreting our results. It can be assumed that even in the early stages of the formation of the adsorbed film the adsorbed atoms form islands which are revealed by the LEED method only in the region $\Theta > 0.2$
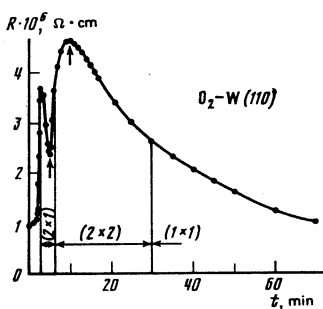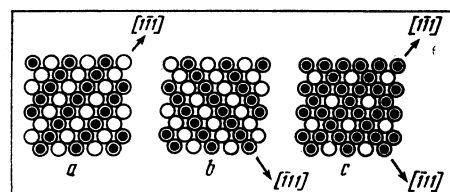

FIG. 3. The change in magnetoresistance of a tungsten plate on adsorption of oxygen; $H = 7.5$ kOe, $T = 4.2$ K. The vertical straight lines show the regions of existence of the $p(2 \times 1)$, (2×2) and $p(1 \times 1)$ structures. The vertical arrows indicate the maximum development of these structures.

FIG. 5. Schematic representation of surface diffraction lattices formed by oxygen atoms (dark circles) on a tungsten (110) face; a and b—$p(2 \times 1)$ structure corresponding to $\Theta = 1/2$, c—(2×2) structure for $\Theta = 3/4$.

(Ref. 29). It was shown by subsequent investigations that apart from growth of $p(2 \times 1)$ islands, statistical filling of free gaps by oxygen atoms takes place, and only in the region of $\Theta = \frac{1}{2}$ does the system assume a homogeneous form.[30,31] Only this last mechanism can evidently provide the sharp singularity on the $R(t)$ curve. Later on, the increase in the concentration of particles leads to the filling of some remaining places and the formation of the next structure (2×2). As can be seen from Fig. 5c, its unit cell is formed by the vacancy lattice which arise~ ~t $\Theta = \frac{3}{4}$. The final $p(1 \times 1)$ structure merely repeats ι ructure of the substrate face. In this way, simple considerations based on the symmetry of the adsorbed layers enables a Θ scale to be superimposed on the time scale of Fig. 3. The minimum in $R(t)$ corresponds to the concentration $\Theta = \frac{1}{2}$, the $R(t)$ maximum to the concentration $\Theta = \frac{3}{4}$. The remaining time is required for filling-in the monolayer. The asymmetry in the dependence reflects the considerable reduction in condensation coefficient for oxygen as Θ increases.[32]

We shall now consider the possible electron transitions. We immediately note that the diffraction grating formed by monolayer oxygen causes electron transitions to equivalent states. Such transitions are also realized at an atomically pure crystal surface. Transitions which can arise from interaction with the regular $p(2 \times 1)$ or (2×2) structures are more convenient to analyze on a shadow projection of the tungsten Fermi surface onto the (110) plane studied, as shown in Fig. 6. The figure is constructed from the data of Boĭko and Gasparov.[33] The system of diffraction reflections seen on the electron diffraction camera screen is shown, with the corresponding reciprocal lattice points of the structure analyzed which determine the electron transitions at the Fermi surface, i.e., the possible channels for specular reflections. The points corresponding to an incident and reflected electron are here situated on a single straight line ($k_t = $ const or $g = $ const), perpendicular to the plane of the drawing, while the vectors g_1 and g_2 correspond to the diffracting grating.
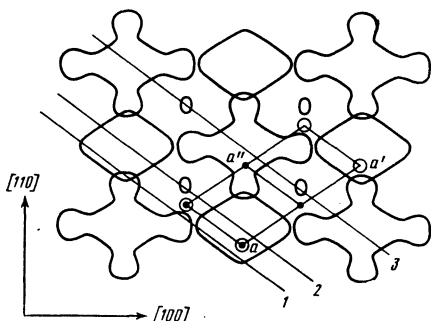

FIG. 6. Shadow projection of tungsten Fermi surface onto the (110) plane, according to data of Boĭko and Gasparov.[33] Possible electron transitions are shown: light circles—for the $p(2 \times 1)$ structure from point a to a'; dark circles—for the (2×2) structure from point a to a''. The narrow regions of phase space where electron–hole umklapp processes are possible even for the $p(2 \times 1)$ structure are indicated by the fine lines 1 and 3.

The method described enables the correlation between the atomic structure of the surface and the behavior of the $R(t)$ dependence to be analyzed.

We shall discuss possible electron transitions in the oxygen + (110) W face for the phase-space point a chosen at random. They are denoted by the open circles for the first regular $p(2 \times 1)$ structure and give the single transition to a' or other points that are multiples of g, i.e., Peierls transitions[34] to physically equivalent points in phase space. The remaining points of the reciprocal lattice do not coincide with any portion of the tungsten Fermi surface and the corresponding transitions do not occur. The thin lines 1–3 in Fig. 6 mark very narrow regions where nonequivalent transitions can, nevertheless, take place and produce umklapp both between the basic parts of the Fermi surface (the electron "jack" and the hole "octahedron") and between hole "ellipsoids" and the remaining parts of the Fermi surface. In particular, electron-hole umklapp processes are possible on lines 1 and 3. Since these regions only occupy a small part of phase space, the $p(2 \times 1)$ structure should mainly give specular reflections.

A different situation can arise on going to the (2×2) structure. The reciprocal-lattice vector is now halved and the translational symmetry period of the W(110) plane is doubled. The reciprocal-lattice points of this structure are indicated by dark circles which can be positioned simultaneously at electron and hole portions of the Fermi surface. The momentum indeterminancy in the tangential direction gives electron-hole umklapp processes between the hole "octahedron" of the Fermi surface and the electron "jack" (the transition from a to a''). Nevertheless, transitions that are multiples of g can also take an electron to equivalent points. As we see, the reflection is two-channel. The final $p(1 \times 1)$ structure only leads to transitions to physically equivalent points of phase space.

Now we shall consider the whole behavior of the $R(t)$ dependence shown in Fig. 3, taking account of the possible nature of the surface reflection of electrons by various periodic structures. We first of all point out the high sensitivity of the magnetoresistance of a thin tungsten plate to the adsorption of monolayer impurity oxygen films. In some cases the relative change ΔR is almost of the same order of magnitude as R. This is in particular due to the high concentration of surface current localized in a layer of the order of r at the boundary of the conductor (r is the Larmor radius). According to our calculation, this is 10^2 to 10^3 times greater than the bulk current density in the specimens studied. As is well known, the skin effect for a dc electric current in compensated metals in a strong magnetic field, $\omega\tau \gg 1$, is due to the considerably different mobilities of electrons in the bulk of the conductor and at its surface.[2] The current in the core of the conductor arises from diffusion of the centers of the orbits of the carriers rotating in the magnetic field along the cyclotron trajectories as a result of infrequent bulk collisions. On the other hand, at the surface each collision with the boundary shifts the electron along the applied electric field by an amount of the order of the radius of the cy-

clotron orbit; the surface mobility and current are thereby appreciably increased.

Recent theoretical studies[17] showed that the surface conductivity of current carriers depends weakly on the nature of electron reflections if the carriers, undergoing sufficiently rapid intragroup mixing, stay within the limits of one branch of the equal-energy surface. For both specular and diffuse reflections, the electrons and holes drift in a magnetic field along the specimen surface with the Fermi velocity v_F. Their drift length along the surface, l_{eff}, is only limited by collisions within the bulk, which lead to departure of the quasi-particles from a subsurface layer of thickness r. In this case $l_{eff} = v_F \tau = l$ and depends weakly on the nature of the reflection. In an electric field such a process takes place with acquisition of energy and momentum. If electron-hole umklapp processes are possible on reflection at the surface, the quasiparticle transfer from electron to hole orbits represents a change in sign of their drift along the applied electric field. Such processes lead to a loss of the energy and momentum acquired in the field, i.e., they are dissipative.

If an umklapp process is entirely probable during the period of the effective path along the surface, then

$$Q > r/l, \qquad (2)$$

where Q is the probability of electron-hole umklapp processes ($0 \leqslant Q \leqslant 1$).

The magnitude of the conduction-electron drift along the surface, averaged over the n channels of specular reflection

$$\Delta x = \left\langle \sum_{i,k}^{n} (\Delta x_i + \Delta x_k) \right\rangle,$$

determines the effective mean free path of the quasiparticles l'_{eff}. If criterion (2) is satisfied, the quantities $\Delta x_{i,k}$ have different signs since the electrons and holes drift in different directions and l'_{eff} becomes less than $l_{eff} = l$. The contribution of the electrons to the surface conductivity, proportional to the coefficient of particle diffusion over the surface, $\sigma \sim D = (l'_{eff})^2 / \tau$, is then small. We note that in our experiment the quantity r/l according to calculation is 10^{-2} to 10^{-3}, so that even a small probability Q can essentially determine the surface conductivity of the specimen. It can be concluded that in a sufficiently strong magnetic field the form of the $R(t)$ curve (Fig. 3) is mainly determined by the probability Q of electron-hole umklapp processes. We shall consider the curve shown in Fig. 3 from this point of view.

The first maximum in the region $\Theta < \frac{1}{2}$ can be ascribed to a structureless form of oxygen. It gives isotropic diffuse reflections with transitions to all parts, including isolated parts, of the Fermi surface. The reflections of electrons become ever more specular with the development of the $p(2 \times 1)$ phase. The depth of the minimum in R, which corresponds to the maximum development of the $p(2 \times 1)$ structure, is determined by some "residual" diffuseness. In fact, the film is not uniform since it consists of domains with different orientations (see Fig. 5); besides, even a uniform $p(2 \times 1)$ film can

FIG. 7. Development of out-of-register structure for the oxygen-tungsten system: a—surface covered with an ordered oxygen monolayer film, b and c—surface of crystal heated to $T > 800$ K; in diffraction picture b domains of only one orientation can be seen, in picture c—there are domains in two equivalent orientations in the beam. Electron beam energy $E = 30$ eV.

cause some admixture of recombination processes. The corresponding narrow parts of phase space are shown by straight lines 1 and 3 in Fig. 6.

Diffraction of electrons by the next (2×2) structure, first of all, produces Peierls transitions to equivalent states and, secondly, brings about electron-hole recombination between the main parts of the Fermi surface. Such surface reflection can be characterized as two-channel specular reflection. A small probability Q can give a noticeable contribution to the magnetoresistance of a plate ($\Delta R \sim R$) even if it is accepted that the dominant processes are Peierls transitions. Finally, the transition to a matched monolayer produces only single-channel specular reflections (i.e., Peierls transitions) and leads to a reduction in R down to the initial value for a clean surface.

A characteristic feature of the oxygen-tungsten system at $\Theta \approx 1$ is the possibility of some compacting of the oxygen monolayer and a change in the angles of the unit cell of the surface lattice. Such rearrangement processes take place at temperatures $T > 800$ K and can be the initial stages of oxidation of the surface and its reconstruction. As a result of this, the two-dimensional surface lattice goes out of register relative to the tungsten lattice.[28,35,36] The corresponding change in the diffraction pattern after heating the oxygen film is shown in Fig. 7. The first picture corresponds to a surface covered up to a monolayer of atomic oxygen; it does not differ from a Laue picture for a clean surface. Gradual increase in the temperature leads to the appearance of a system of diffraction reflections along the $\langle 13 \rangle$ direction and corresponding to the out-of-register structure. A complicated system of transitions arises in this case, illustrated in Fig. 8. It can be seen that such an out-of-register lattice can both lead to intragroup mixing of carriers and bring about electron-hole umklapp processes. In fact, the sharp increase in magnetoresistance of the plate, which arises as a result of a change of translational symmetry in the ad-
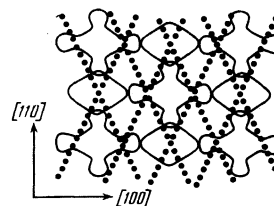

FIG. 8. System of electron transitions for out-of-register structure arising for the oxygen-tungsten system.
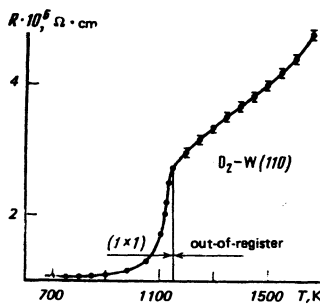
FIG. 9. Heating temperature dependence of magnetoresistance R of plates for the oxygen-tungsten system. The vertical straight lines delineate the regions of existence of the $p(1 \times 1)$ and out-of-register structures.

FIG. 11. Scheme of electron transitions for two possible out-of-register structures b and c, which arise for the silver-tungsten system. The light circles indicate transitions which can give electron-hole umklapp processes, the dark circles give intragroup mixing.

sorbed layer confirms this deduction (Fig. 9). We should point out that the resistance growth is noticeable at temperatures such that the LEED picture still shows no change. The reconstruction of the surface probably already starts under these conditions, but the sensitivity of the LEED method is insufficient for observing it. Further increase of temperature up to $T > 1700$ K leads to a gradual evaporation of the oxygen. The $R(\Theta)$ curve can then be traced in the reverse direction, starting from the region $\Theta < \frac{3}{4}$. For large values of Θ, including the (2×2) structure at $\Theta = \frac{3}{4}$, the surface crystal lattice remains, according to LEED results, noticeably distorted.

Hydrogen-tungsten system. Adsorption of hydrogen was carried out at $T = 4.2$ K since it is easy to attain a monolayer at these temperature. The upper curve (Fig. 10) shows the change in R with exposure time in fixed magnetic field. This dependence is almost bell-shaped and indicates that the hydrogen atoms form an ordered monolayer film even at $T = 4.2$ K. Perfect diffraction pictures, however, arise on heating the system at $T > 50$ K. The lower curve of Fig. 10 shows the corresponding $R(t)$ results for films heated to 200 K. The hydrogen+(110) tungsten system forms the same consecutive $p(2 \times 1)$, (2×2) and $p(1 \times 1)$ structures as the previous oxygen+tungsten system and were also observed earlier[37,38]. As can be seen from the figure, the sticking coefficient for hydrogen stays practically unchanged over the whole Θ range, and the $p(2 \times 1)$ struc-
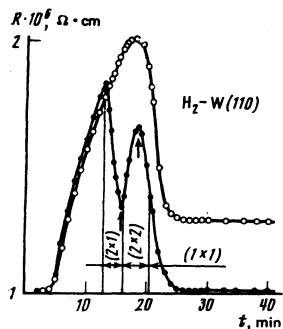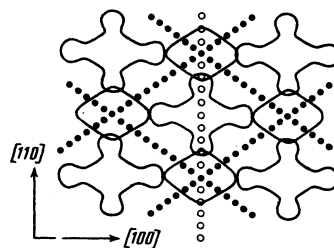
ture at $\Theta = \frac{1}{2}$, corresponding to the minimum in R, actually arises in approximately the middle of the bell-like $R(t)$ curve. The transition to the (2×2) structure is indicated by the distinct maximum. It corresponds to "switched-on" umklapp processes. Finally, the perfect $p(1 \times 1)$ structure gives one-channel specular reflection and a reduction in R to the initial value. The $R(t)$ curve shown in Fig. 10 can be obtained in the reverse order by gradual evaporation of small portions of hydrogen. From a comparison of the experimental results for the two systems studied here it can be concluded that the nature of the reflection of electrons is mainly determined by the symmetry of the adsorbed layers and not by their chemical nature.

Silver-tungsten system. As was shown for oxygen and hydrogen on a W(110) face, an adsorbate which exactly repeats the substrate face structure does not destroy the specular reflection of conduction electrons. The Ag + W (110) system interested us because silver, on the contrary does not exactly repeat the substrate structure. Studies of submonolayer films of silver by the LEED method[39-41] provide evidence of this. The growth of two-dimensional silver crystals on a tungsten surface proceeds in two stages. Initially, at small surface concentration, ordered islands of silver grow with a lattice which is not in register with the tungsten, and the reflection points are oriented in the $\langle 01 \rangle$ direction. As a monolayer is approached a new system of reflections arises which go in another direction. Both orientations exist at intermediate concentrations $0 < \Theta < 1$. It

FIG. 10. Magnetoresistance $R(t)$ of plates on adsorption of hydrogen. The regions of existence of the regular $p(2 \times 1)$, (2×2) and $p(1 \times 1)$ structures are shown. The upper curve was obtained on adsorption of hydrogen on a crystal cooled to 4.2 K.
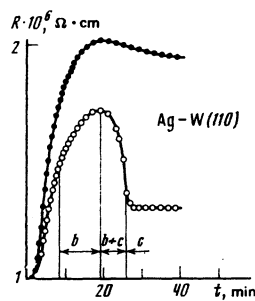

FIG. 12. Change in magnetoresistance on adsorption of silver: b—region of existence of the structure which gives umklapp processes; c—region of existence of the structure which gives only intragroup mixing; b +c the region where the b and c phases coexist.

is significant that the transition from one type of island to the other indicates rotation of the reciprocal lattice of the adsorbed film relative to the axes of the substrate crystal.[41]

Figure 11 shows reflections for both types of out-of-register structures we observed, superimposed on a shadow projection of the Fermi surface. It can be seen that the first type of electron transition b, shown by the open circles, can cause both intragroup diffusive mixing of quasiparticles and "switching-on" of electron-hole umklapp processes. The second type of transition c, indicated by black circles, differs in that the chains of points only pass through either electron or hole sections of the Fermi surface, except for narrow regions of phase space indicated by lines 1, 2 and 3 in Fig. 6. The $R(t)$ dependence for the silver-tungsten system is shown in Fig. 12. The upper curve corresponds to silver deposited on a crystal surface cooled to 4.2 K; the silver film is then structureless. The lower curve was obtained as a result of heating the adsorbed film to 500 K. Heating leads to the appearance of diffration pictures corresponding to out-of-register structures. The vertical straight lines indicate the region of existence of these diffraction pictures. It can be seen that structure b which "switches-on" electron-phonon umklapp processes corresponds to the magnetoresistance maximum. The resistance falls in the region of co-existence of the two types of structure $b + c$. As the silver concentration increases, the b phase goes over into c and the value of R falls smoothly to the value R_{min} and then remains unchanged. The magnitude of R_{min} is determined by electron-hole umklapp processes in narrow regions of phase space.

The observed correlation found for all the systems studied between magnetoresistance and the structures of oxygen, hydrogen and silver submonolayer films thus enables conclusions to be drawn about the determining influence of translational symmetry on the nature of the reflection of conduction electrons at a metal surface. The chemical nature of the adsorbed atoms is revealed in the structural properties of the adsorbed layer itself.

It has been shown that the increase in magnetoresistance in the case of the formation of an ordered (2×2) structure is brought about by the "switching-on" of electron-hole umklapp processes.

[1]M. Ya. Azbel', Zh. Eksp. Teor. Fiz. 44, 983 (1963) [Sov. Phys. JETP 17, 667 (1963)].

[2]V. G. Peschanskii and M. Ya. Azbel', Zh. Eksp. Teor. Fiz. 55, 1980 (1968) [Sov. Phys. JETP 28, 1045 (1969)].

[3]O. A. Panchenko and P. P. Lutsishin, Zh. Eksp. Teor. Fiz. 57, 1555 (1969) [Sov. Phys. JETP 30, 841 (1970)].

[4]P. P. Lutsishin, O. A. Panchenko, and A. A. Kharlamov, Zh. Eksp. Teor. Fiz. 64, 2148 (1973) [Sov. Phys. JETP 37, 1083 (1973)].

[5]O. A. Panchenko, P. P. Lutsishin, and Yu. G. Ptushinskiĭ, Zh. Eksp. Teor. Fiz. 66, 2191 (1974) [Sov. Phys. JETP 39, 1079 (1974)].

[6]A. A. Kharlamov, O. A. Panchenko, and I. N. Yakovkin, Zh. Eksp. Teor. Fiz. 71, 760 (1976) [Sov. Phys. JETP 44, 401 (1976)].

[7]A. A. Mitryaev, O. A. Panchenko, and J. J. Razgonov, Surf. Sci. 75, 376 (1978).

[8]S. I. Bozhko, A. A. Mitryaev, O. A. Panchenko, I. I. Razgonov, and V. S. Tsoĭ, Fiz. Nizk. Temp. 5, 739 (1979) [Sov. J. Low Temp. Phys. 5, 351 (1979)].

[9]J. P. Chauvineau and C. Pariset, Surf. Sci. 36, 155 (1973).

[10]A. M. Grishin, P. P. Lutsishin, Yu. S. Ostroukhov, and O. A. Panchenko, Zh. Eksp. Teor. Fiz. 76, 1325 (1979) [Sov. Phys. JETP 49, 673 (1979)].

[11]A. F. Andreev, Usp. Fiz. Nauk 105, 113 (1971) [Sov. Phys. Usp. 14, 609 (1971)].

[12]R. F. Green, In: Solid State Surface Science, M. Green (Ed) Vol. 1, Dekker, New York (1970).

[13]V. S. Tsoĭ and Yu. A. Kolesnichenko, Zh. Eksp. Teor. Fiz. 78, 2041 (1980) [Sov. Phys. JETP 51, 1027 (1980)].

[14]V. G. Peschanskii, V. Kardenas, M. A. Lur'e, and K. Yasemidis, Zh. Eksp. Teor. Fiz. 80, 1645 (1981) [Sov. Phys. JETP 53, 849 (1981)].

[15]A. O. Panchenko, A. A. Kharlamov, and Yu. G. Ptushinskiĭ, Zh. Eksp. Teor. Fiz. 67, 780 (1974) [Sov. Phys. JETP 40, 386 (1975)].

[16]O. V. Kirichenko, V. G. Peschanskiĭ, and S. N. Savel'eva, Zh. Eksp. Teor. Fiz. 77, 2045 (1979) [Sov. Phys. JETP 50, 976 (1979)].

[17]A. I. Kopeliovich, Zh. Eksp. Teor. Fiz. 78, 987 (1980) [Sov. Phys. JETP 51, 498 (1980)].

[18]P. P. Lutsishin, T. N. Nakhodkin, O. A. Panchenko, and Yu. G. Ptushinskiĭ, Pis'ma Zh. Eksp. Teor. Fiz. 31, 599 (1980) [JETP Lett. 31, 563 (1980)].

[19]P. J. Estrup and E. G. McRae, Surf. Sci. 25, 1 (1961).

[20]J. A. Becker, E. J. Becker, and R. Brandes, J. Appl. Phys. 32, 411 (1961).

[21]Yu. P. Gaĭdukov, E. M. Golyamina, and N. P. Danilova, Pis'ma Zh. Eksp. Teor. Fiz. 22, 231 (1975) [JETP Lett. 22, 107 (1975)].

[22]T. N. Nakhodkin, O. A. Panchenko, and G. M. Pugach, Fiz. Tverd. Tela (Leningrad) 20, 1589 (1978) [Sov. Phys. Solid State 20, 921 (1978)].

[23]A. A. Mitryaev, O. A. Panchenko, and G. M. Pugaev, Zh. Eksp. Teor. Fiz. 75, 1356 (1978) [Sov. Phys. JETP 48, 683 (1978)].

[24]E. A. Wood. J. Appl. Phys. 35, 1306 (1964).

[25]E. Bauer, Suf. Sci. 7, 351 (1967).

[26]M. A. Van Hove and S. Y. Tang, Phys. Rev. Lett. 35, 1092 (1975).

[27]J. C. Buchholz, G. G. Wang, and M. G. Lagally, Surf. Sci. 49, 508 (1975).

[28]V. E. Bezvenyuk, V. A. Ishchuk, Yu. G. Ptushinskiĭ, and A. G. Fedorus, Fiz. Tverd. Tela (Leningrad) 21, 1273 (1979) [Sov. Phys. Solid State 21, 739 (1979)].

[29]J. C. Tracy and J. M. Blakely, Surf. Sci. 15, 257 (1969).

[30]G. Ertl and M. Plancher, Surf. Sci. 48, 364 (1975).

[31]T. Engel, H. Niehus, and E. Bauer, Surf. Sci. 52, 237 (1975).

[32]V. S. Bosov and B. A. Chuĭkov, Ukr. Fiz. Zh. 18, 1568 (1973).

[33]V. V. Boĭko and V. A. Gasparov, Zh. Eksp. Teor. Fiz. 61, 2362 (1971) [Sov. Phys. JETP 34, 1266 (1972)].

[34]R. E. Peierls, Quantum Theory of Solids, Clarendon Press, Oxford (1955).

[35]D. A. Gorodetskiĭ, Yu. P. Mel'nik, and A. A. Yas'ko, Ukr. Fiz. Zh. 12, 970 (1967).

[36]E. Bauer and T. Engel, Surf. Sci. 71, 695 (1978).

[37]K. J. Matysik, Surf. Sci. 29, 324 (1972).

[38]V. V. Gonchar, O. V. Kanash, A. G. Naumovets, and A. G. Fedorus, Pis'ma Zh. Eksp. Teor. Fiz. 28, 358 (1978) [JETP Lett. 28, 330 (1978)].

[39]D. A. Gorodetskiĭ and Fung-Kho, In: Physics of Metal Films [in Russian] 26, 53, Kiev (1969).

[40]E. Bauer and H. Poppa, Thin Solid Films 12, 167 (1972).

[41]E. Bauer, H. Poppa, G. Todd, and P. R. Davis, J. Appl. Phys. 48, 3773 (1977).

Translated by R. Berman

765   Sov. Phys. JETP 55(4), April 1982

Lutsishin et al.   765